Deutscher Luft- und Raumfahrtkongress 2021
DocumentID: 550236

ASSESSMENT OF THE HANDLING QUALITIES OF MULTIROTOR CONFIGURATIONS USING REAL TIME SIMULATION

Kagan Atci, Michael Jones, Tim Jusko
German Aerospace Center (DLR), Institute of Flight Systems (FT)
Lilienthalplatz 7, 38108 Braunschweig, Germany

Abstract

The popularity of the electric vertical take-off and landing (eVTOL) aircraft in the Urban Air Mobility (UAM) market has significantly increased over the last decade. Many institutes and companies around the globe are conducting research in this field to translate the theory into practice by developing novel eVTOL configurations. At the German Aerospace Center, the Institute of Flight Systems has been developing processes not only to model novel configurations, but also to asses them qualitatively with real pilots. In this regard, a study concerning the Handling Qualities (HQs) assessments of a two passenger quadrotor configuration with variable blade pitch and variable rotor rotational speed control was conducted. The simulation tests were performed in DLR's Air VEhicle Simulator (AVES), where the HQs were assessed through Mission Task Elements (MTEs) taken from ADS-33E-PRF. Results from the study showed critical HQs issues regarding the control sensitivity, vehicle stability and yaw bandwidth.

Keywords

Urban Air Mobility; eVTOL; Multirotor; Quadrotor; Flight Dynamics; Handling Qualities

NOMENCLATURE

Symbols

cmd	vehicle control command	$\%$
Ω	rotor rotational speed	rpm
Ψ	rotor blade rotation angle	$^\circ$
Θ	swashplate collective pitch	$^\circ$
η	rel. spanwise coordinate	$-$
I_{xx}	moment of inertia in long. axis	$\mathrm{kg\,m^2}$
I_{yy}	moment of inertia in lat. axis	$\mathrm{kg\,m^2}$
I_{zz}	moment of inertia in vertical axis	$\mathrm{kg\,m^2}$
L_p	roll accel. from roll rate	$\mathrm{rad/s}$
L_v	roll accel. from lateral velocity	$\mathrm{rad/m\,s}$
M_q	pitch accel. from pitch rate	$\mathrm{rad/s}$
M_u	pitch accel. from long. velocity	$\mathrm{rad/m\,s}$
N_r	yaw accel. from yaw rate	$\mathrm{rad/s}$
ϕ, θ, ψ	roll, pitch, yaw angle	$^\circ$
p, q, r	roll, pitch, yaw rate	$^\circ\mathrm{/s}$
R	rotor thrust command	Θ or Ω
u, v, w	translational velocities	$\mathrm{m/s}$
V_H	horizontal speed over ground	$\mathrm{m/s}$
X_q	longitudinal accel. from pitch rate	$\mathrm{m/rad\,s}$
X_θ	longitudinal accel. from pitch	$\mathrm{m/s^2}$
X_u	longitudinal accel. from long. velocity	$\mathrm{1/s}$
Y_p	lateral accel. from roll rate	$\mathrm{m/rad\,s}$
Y_ϕ	lateral accel. from yaw attitude	$\mathrm{m/s^2}$
Y_v	lateral accel. from lateral velocity	$\mathrm{1/s}$
Z_w	heave accel. from heave velocity	$\mathrm{1/s}$

Indices

C	collective
P	longitudinal cyclic
R	lateral cyclic
Y	pedal

1. INTRODUCTION

In recent years, the interest in electric vertical take-off and landing aircraft (eVTOL)[1] has increased, thanks to the new confidence in advancing technologies,

[1]The term eVTOL is often used interchangeably with other names, including Urban Air Mobility (UAM) and Advanced Air Mobility (AAM).

doi: 10.25967/550236

such as battery, material, control & automation, and design & analysis [1]. Since the market is still gaining momentum, a 32 billion-dollar capacity for the UAM market is estimated with 23.000 flying eVTOLs by 2035 [2]. Despite the promising reduced emissions, safer transportation, and connected mobility, there are still significant challenges that must be addressed prior to eVTOL emerging as a viable form of transportation.

To this date, a wide range of eVTOL concepts have been proposed, while a handful of concepts, such as Volocopter 2X, Airbus CityAirbus and EHang 184 are already flying. Depending on the concept of operations (CONOPS) proposed by the manufacturers, eVTOL concepts differ from each other. Some vehicles, for example, are designed only for the low speed flight and reflect typical rotorcraft features, while others are designed with focus on the forward flight regime by hybridizing rotorcraft and fixed wing, concentrating on the shortened journey time. Three main concept groups can be distinguished in this regard: Multirotors, Lift+Cruise and Tilt-X [2].

Most of the current eVTOL studies concentrate on the multirotor concepts. Unlike in the conventional main rotor-tail rotor configuration, multirotors have a vertical thrust system that is distributed over multiple rotors in smaller size. Typical helicopters utilize blade pitch to control the vehicle about all axes, which is achieved through the use of a swashplate at a constant rotor rotational speed. In multirotor concepts, the vehicle maneuver is often controlled through changing the lift in individual rotors. Two variants are available for the rotor lift control: one is the variable blade pitch, and the other is the variable rotational speed with the blades at fixed pitch angle. Here, the latter offers the benefit of reduced mechanical complexity compared to the former using electric motors. Some significant benefits are reduced vehicle mass (and therefore smaller rotors) [3], and reduced operating and maintenance costs [4].

As eVTOL vehicles increase in load capacity , so does the rotor size. The increase in the rotor size would lead to higher rotational inertia of the rotors, causing to longer response times for the control of the rotor rotational speed. The lag in the rotor response reduces the benefit offered by the use of variable rotor speed control [5]. Therefore, collective controlled quadrotors exhibit more stable flight dynamics in closed loop control than the rotational speed controlled rotors for the eVTOLs used in passenger transportation [6].

At the German Aerospace Center (DLR), ongoing works are focused on the parametric design and assessments of multirotor configurations in two variants: one is a quadrotor concept and the other is a new medical personnel deployment vehicle, consisting of four main rotors and two pusher propellers. As the works are still in development, it is intended to perform future studies in the multidisciplinary rotorcraft conceptual design environment IRIS [7] developed by the Institute of Flight Systems.

Although many studies have been conducted to investigate flight characteristics of multirotors, a piloted approach towards the Handling Qualities (HQs) of the mentioned rotor control variants is still a remaining issue. This work aims to provide a framework for assessing the HQs of multirotor configurations in a piloted real time flight simulation environment. For the showcase, a two passenger quadrotor vehicle with collective controlled (COL) and rotor rotational speed controlled (RPM) variants taken from the literature study [3, 6] was remodeled and modified. Prior to HQ assessments, both variants were analyzed in terms of flight performance and flight dynamics. After these analysis, HQs were assessed using criteria and mission task elements (MTEs) provided by ADS-33E-PRF (*ADS-33 in short*) [8] in a full-scale flight simulator with experienced helicopter pilots.

The paper proceeds as follows. First, the process approach is introduced, outlining the framework steps from flight model creation to quantitative and qualitative analysis of the studied quadrotors. Second, the mathematical theory of the quadrotor bare airframe vehicle control using conventional helicopter inceptors is introduced. This is followed by the desktop analysis, revealing the trim performance and flight dynamics of the studied models. Following, the results of the HQs investigations are elaborated covering the predicted and awarded HQs ratings resulted from the piloted simulations. Finally, conclusions and outlook of the study are given.

2. PROCESS APPROACH

The process incorporates automated steps in a framework to reduce the necessary user interaction, saving time and effort. As shown in Fig. 1, the assessment process takes place in three steps: *Parameterization*, *Modeling*, and *Analysis*. These steps are described in following sections.

2.1. Parameterization

The quadrotor models were generated based on the data given in [3]. The missing parameters in the baseline models were complemented with additional data for the cell, rotor, blade and fuselage modeling. The final modeling parameters are shown in Table 1, where Fig. 2 depicts a visualization of the configuration studied.

For the mass and inertial computations, the center of gravity (CG) was assumed to be located at the geometrical middle point of the fuselage. Thus, the change in moment that result from CG offset were neglected.

The rotors were positioned equidistantly in lateral and longitudinal directions around the CG with no tilting.

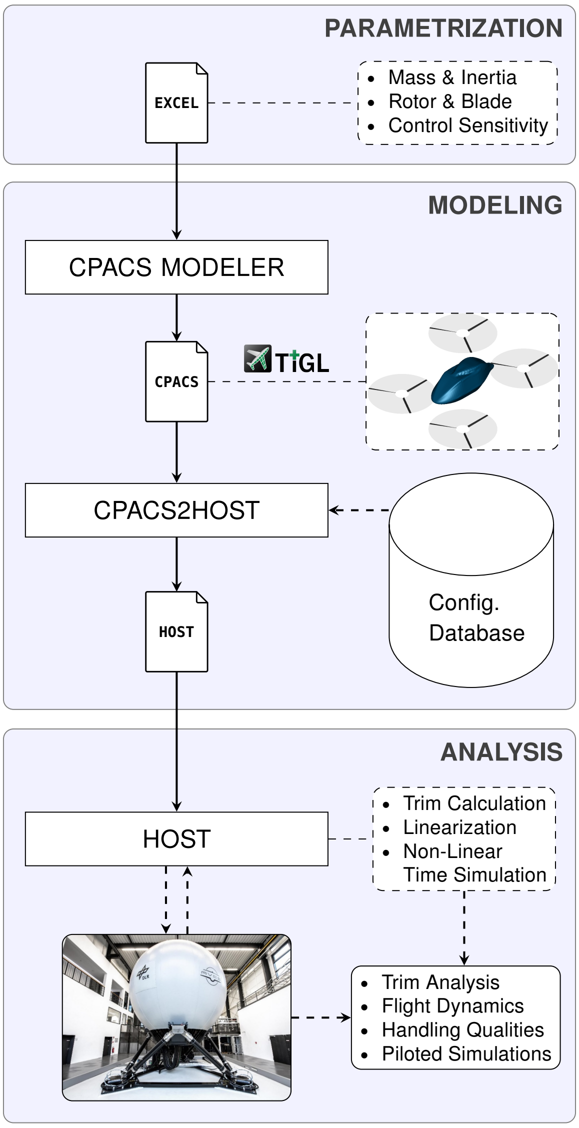

Figure 1 Framework process flow

Parameter	Unit	COL	RPM
CELL			
Gross Mass	kg	1248	1039
I_{xx}	$\mathrm{kg\,m^2}$	4150	2878
I_{yy}	$\mathrm{kg\,m^2}$	4150	2878
I_{zz}	$\mathrm{kg\,m^2}$	5021	3482
FUSELAGE			
Length*	m	6,3	6,3
Width*	m	2,36	2,36
Heigth*	m	2,1	2,1
ROTOR			
Radius	m	2,59	2,38
Rotation Speed	rpm	615,0	624,6
Blade Number	–	3	3
Mass	kg	16,82	13,40
Inertia	$\mathrm{kg\,m^2}$	56,4	37,94
Lock Number	–	3,88	3,65
Rotor Positioning*			
a - Lat. rotor gap	–	0,25	0,25
b - Rear rotor z-pos.	m	0,9	0,9
c - Vert. rotor spacing	–	0,9	0,9
d - Long. rotor gap	–	0,25	0,25
BLADE			
Chord	m	0,149	0,137
Root Twist*	°	35	35
Twist Slope*	°/m	-16,9	-18,4

Table 1 Design parameters of the quadrotor configurations
** identifies the complemented parameters*

This way, all rotors would produce same amount of moment about x- and y- axis, given equal thrust in hover. Here, the positioning of the rotor centers were considered as rotor radius added to a rotor gap that resulted from a factor multiplied with the rotor radius. These factors are given as a for the lateral positioning and d for the longitudinal positioning in Fig. 2 and Table 1. Furthermore, the forward and aft rotors were vertically separated for achieving better flight performance. For example, [6] shows that such modification can enable power reductions up to 4.5% in forward flight. The vertical rotor separation was performed using two steps. Initially, the aft-rotors were positioned with respect to the CG by b. Following, the lower rotors were positioned in a distance determined by the separation factor c multiplied with the rotor radius (see Fig. 2a).

Each rotor has three blades with a rectangular planform and linear geometric twist. The root cutout was set to $\eta = 0.2$ relative span in each blade. The root profile was positively twisted by 35°. The twist slope was selected at such a rate that the twist angle at the tip profile is neutralized. As for the aerodynamic blade section, the NACA 23012 was chosen, which is an airfoil widely used in the rotor blade design.

The fuselage aerodynamics were modeled using the polars of ACT/FHS scaled to the drag area of the quadrotor fuselage.

2.2. Modeling

Initializing the automated framework, the modeler script creates a CPACS file [9] with the data imported from the Excel table, configuring the quadrotor in a finer level of detail. The CPACS file contains all the necessary data to create the flight model. Moreover, the vehicle geometry can be visualized using TIGL library [10] parsing the CPACS file.

The flight models are derived in the form of HOST [11] model files (more information to HOST in the following section). These model files interpret the constituting

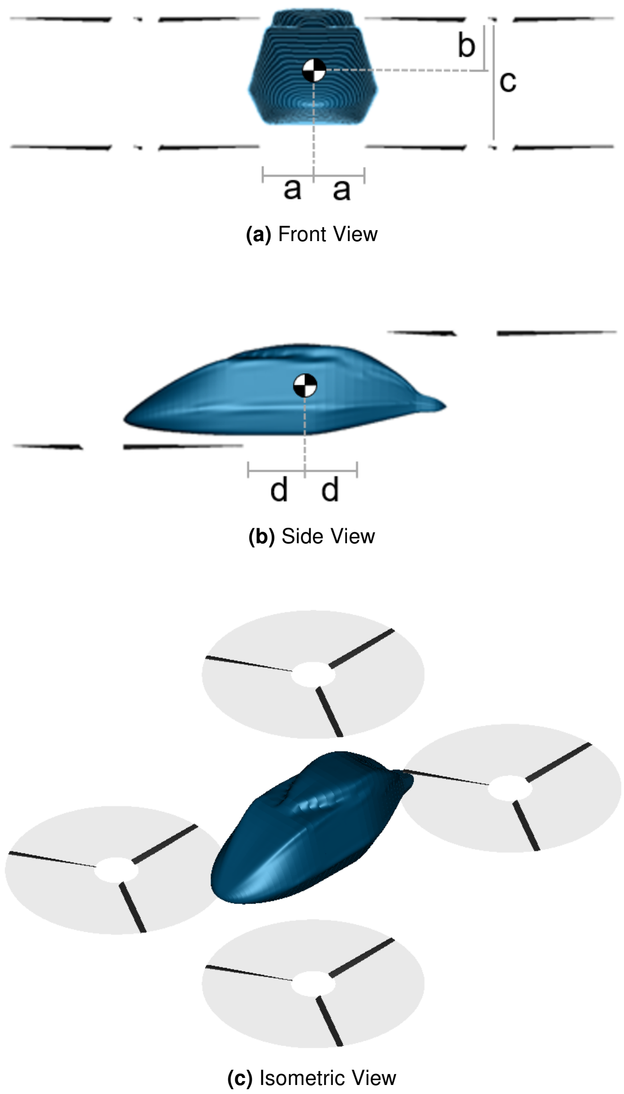

Figure 2 Visualization of the 2-passenger quadrotor model

elements of the rotorcraft, such as rotor, blade, aerodynamic and inertial data. The complexity of the model structures in HOST requires a comprehensive generic approach in creating the model files with the data transferred from the CPACS file. For this purpose, a new object oriented tool named CPACS2HOST was developed, which creates flight models of rotorcraft configurations for HOST by parsing CPACS files. When a new configuration is studied, the user defines a template model architecture representing the configuration in a separate XML file, referred to as the configuration database. During *Modeling*, CPACS2HOST writes the model files based on the configuration architecture imported from the configuration database with the technical data delivered through the CPACS file. This approach enables users to apply rapid changes not only on the model parameters, but also on the configuration features, such as rotor number, modeling detail (e.g. momentum theory or blade element theory), or control variant (collective or rpm), while significantly simplifying the entire process.

2.3. Analysis

For the flight dynamics analysis, a sophisticated helicopter simulation tool called HOST is used. HOST embodies three main functions on flight model analysis: trim, non-linear time simulation and equivalent linear system computation [11]. Thanks to it's generic modeling structure, physical models of various rotorcraft configurations can be created as mentioned in the previous section. Hence, the created flight models for HOST are not only used in the the desktop analysis, but also in the piloted simulations.

The piloted simulations are performed in Air VEhicle Simulator (AVES) [12] in Braunschweig. AVES is a purpose-built research simulation facility maintained and operated by DLR. The simulator features a replica cockpit of the ACT/FHS, DLR's fly-by-light experimental aircraft, which is a highly modified version of the EC135 helicopter. With a field view of 240° and running on a motion platform, AVES offers a high-level hardware for further exploration of the dynamic interaction between the pilot and the rotorcraft. A real time version of HOST is used in AVES for the simulation. Hence, flight models are directly linked to AVES in piloted test campaigns, enabling rapid switch between the models tested.

3. VEHICLE CONTROL

Unlike the conventional main rotor-tail rotor configuration, the control of the quadrotor employs the differential thrust on 4 rotors in order to initiate a maneuver. Therefore, new relations between the conventional inceptor layout and individual rotor control are needed. In following, these relations will be elaborated based on a linear equation system.

Fig. 3 shows the top view of a quadrotor configuration with cross-arrangement. Rotors 1 and 2 rotate in counter-clockwise direction, whereas rotors 3 and 4 rotate in clockwise direction, to cancel the yaw moments. Depending on the desired motion, the quadrotor is controlled by varying the thrust command R of individual rotors. For the RPM-variant, the thrust command R corresponds to the rotor speed Ω, whereas for the COL-variant, the thrust command R is defined by the swashplate collective angle Θ. In both cases, the thrust command acts in the same direction.

Table 2 shows the relation between the positive control inputs and their impact on the thrust command of each rotor. Here, positive collective input leads to increase in the thrust commands in all four rotors equally, in order to heave. To yaw in positive ψ sense, thrust commands in diagonal rotors 3 and 4 are increased, whereas 1 and 2 are decreased. To roll the quadrotor in positive ϕ sense, rotors 2 and 3 increase thrust, as rotor 1 and 4 decrease. Similarly, increasing the thrust in rotors 1 and 3, and decreasing the thrust in rotors 2 and 4 leads to a pitch motion in positive θ sense. It should be noted that the positive θ in the given coordinate system indicates a nose-up attitude, which sets the aircraft in backward motion.

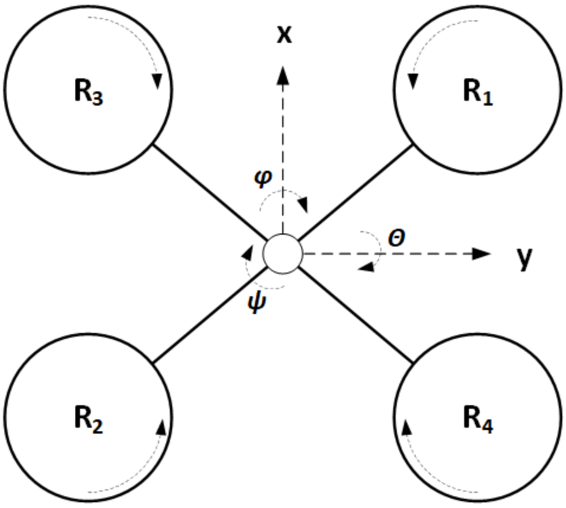

Figure 3 Quadrotor Cross Configuration Scheme (z-direction into the plane)

The relation between the thrust command and the control inputs regarding the desired control sensitivity and neutral position was modeled as a linear system of equations as shown in Eq. (1).

$$\overbrace{\begin{bmatrix} R_1 \\ R_2 \\ R_3 \\ R_4 \end{bmatrix}}^{\overline{R}} = \overbrace{\boldsymbol{\Delta}\,\mathbf{G}\,\overline{C}}^{\overline{R_c}} + \overbrace{\begin{bmatrix} R_{0,1} \\ R_{0,2} \\ R_{0,3} \\ R_{0,4} \end{bmatrix}}^{\overline{R_0}} \tag{1}$$

The rotor thrust command vector $\overline{R}$ is obtained by adding the thrust resulting from the control input $\overline{R_c}$ to nominal thrust $\overline{R_0}$. The control input vector consists of three terms: the control input vector $\overline{C}$ (Eq. (2)), the control authority (gain) matrix $\mathbf{G}$ (Eq. (3)), and the actuator direction matrix $\boldsymbol{\Delta}$ (Eq. (4)).

$$\overline{C} = \begin{bmatrix} cmd_C \\ cmd_R \\ cmd_P \\ cmd_Y \end{bmatrix} \tag{2}$$

$$\mathbf{G} = \begin{bmatrix} g_{1,C} & -g_{1,R} & g_{1,P} & -g_{1,Y} \\ g_{2,C} & g_{2,R} & -g_{2,P} & -g_{2,Y} \\ g_{3,C} & g_{3,R} & g_{3,P} & g_{3,Y} \\ g_{4,C} & -g_{4,R} & -g_{4,P} & g_{4,Y} \end{bmatrix} \tag{3}$$

$$\boldsymbol{\Delta} = \begin{bmatrix} \Delta_1 & 0 & 0 & 0 \\ 0 & \Delta_2 & 0 & 0 \\ 0 & 0 & \Delta_3 & 0 \\ 0 & 0 & 0 & \Delta_4 \end{bmatrix} = \begin{cases} \mathrm{diag}\left(1, \quad 1, \quad 1, \quad 1\right) & \text{for COL,} \\ \mathrm{diag}\left(-1, \quad -1, \quad 1, \quad 1\right) & \text{for RPM} \end{cases} \tag{4}$$

	ΔR_1	ΔR_2	ΔR_3	ΔR_4
Heave	+	+	+	+
Roll	-	+	+	-
Pitch	+	-	+	-
Yaw	-	-	+	+

Table 2 Effects of the positive command inputs on the rotor thrust commands (vice versa for the negative input)

$\mathbf{G}$ represents the sensitivity of the control inputs by defining the maximum allowed thrust command acting on the individual rotors. The vector multiplication of $\mathbf{G}$ with $\overline{C}$ yields the magnitude of the thrust command on each rotor converted from the control positions. With the signs applied from Table 2, the first index of the elements g indicate the rotor number, and the second index indicate the control input. Here, tuning the values high in $\mathbf{G}$ would make the controls more agile, where in contrast, tuning the values down would yield a sluggish flight control. For the COL-variant, the matrix elements are parameterized with respect to blade pitch Θ, whereas in the RPM-variant, these elements are parameterized with respect to rotor rotational speed Ω. As the rpm-controlled rotor pairs 3 and 4 rotate in counter clockwise, the thrust commands acting on those rotors have to be multiplied by -1. In this regard, direction coefficients employed for both control types are given in Eq. (4).

The nominal thrust vector $\overline{R_0}$ represents the command acting on the rotors when all control inputs are canceled ($\overline{C} = \overline{0}$). Given the thrust needed for a certain flight condition, for example at hover, the nominal thrust command at each rotor can be determined by reshaping Eq. (1) with respect to $\overline{R_0}$:

$$\overline{R_0} = \overline{R} - \overline{R_c} \tag{5}$$

Another aspect of the vehicle control is the calibration of the neutral positions of the control elements. For the case of this study, the bare airframe quadrotor model has to be controllable in AVES. Fig. 4 shows the neutral positions of flight controls used in AVES for the trimmed hover state under ideal conditions.

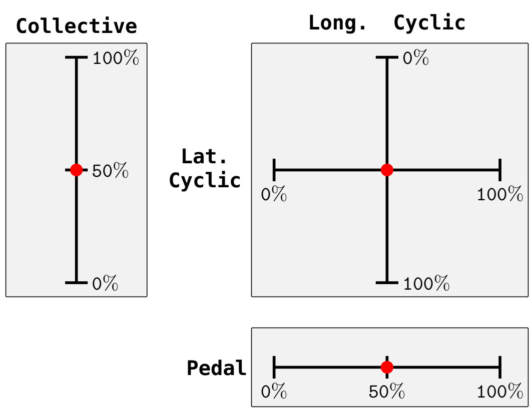

Figure 4 Flight control positions in ideal hover

Here, the borders of the control inputs are defined between 0% and 100%, where the neutral position is placed at 50%, marked with red dots. For this case, Eq. (5) is solved with the control input vector in $\overline{R_c}$ being set to $\overline{C} = \begin{bmatrix} 0.5 & 0.5 & 0.5 & 0.5 \end{bmatrix}^{\mathsf{T}}$. It should be noted that deviations in the collective input cmd_C from 0.5 is possible depending on the flight conditions, as it doesn't pose a violation for the symmetrical flight conditions.

4. DESKTOP ANALYSIS

4.1. Trim

The trim analysis was made with respect to the horizontal flight speed over ground, sweeping from 0 km/h to 200 km/h at 200 m above mean sea level under international standard atmospheric conditions. The results were evaluated in terms of vehicle attitude, total power, and command input.

Fig. 5 shows the roll and pitch attitude of the collective and speed controlled variants. Thanks to the symmetry of the quadrotor, results yield a horizontal flight with no roll attitude for both variants at all trim points. In hover, both variants exhibit a pitch-free attitude, due to the symmetrical rotor arrangement. With increasing horizontal speed, the need for vectoring the rotor thrust emerges in order to create a force in flying direction and cancel out the drag. This is achieved, as the aircraft settles into a nose-down attitude (negative pitch) during the forward flight. In the RPM-variant, a constant linear build-up in the pitch angle can be observed, whereas in the COL-variant, the curve shows a non-linear characteristic. This can be related to the lift experienced on the rotor blades. For the RPM-variant this relation is depended on θ and Ω, whereas for the COL-variant, it is depended on θ and Θ.

The performance curves are plotted in Fig. 6. Here, the difference in the mass and therefore in the rotor dimensions between both variants can be observed, as the COL-variant requires higher power than the RPM-variant. Despite the offset, both curves exhibit similar characteristics. Starting with hover, the required power decreases until about 75 km/h for both variants, as the induced power constantly decreases. As of this point, the parasite drag caused by the fuselage starts to dominate resulting an increase in the required power.

Control inputs are shown in Fig. 7. The collective command is trimmed closed to 50%, whereas the longitudinal cyclic is trimmed exactly at 50% for both variants in hover. Thanks to the symmetrical flight conditions, roll and yaw commands remain at a constant 50% for both variants at all trim points.The control input results confirm that Eq. (1) provides a resilient control of the bare airframe in AVES, when used with well-tuned parameters in the $\mathbf{G}$ matrix.

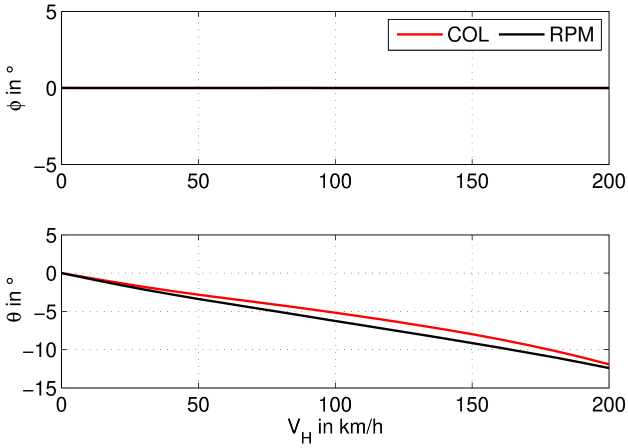

Figure 5 Roll & pitch attitude versus horizontal flight speed

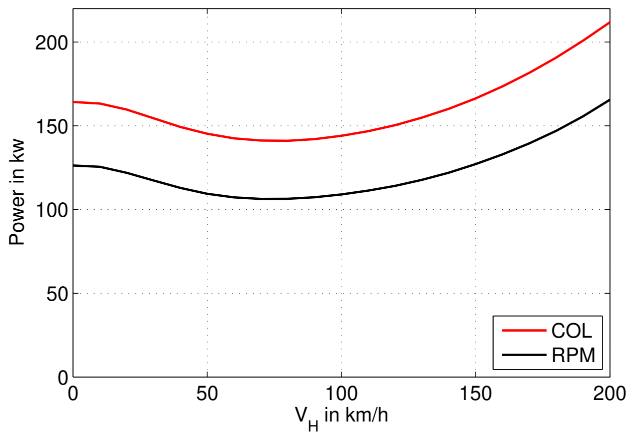

Figure 6 Total power required versus horizontal flight speed

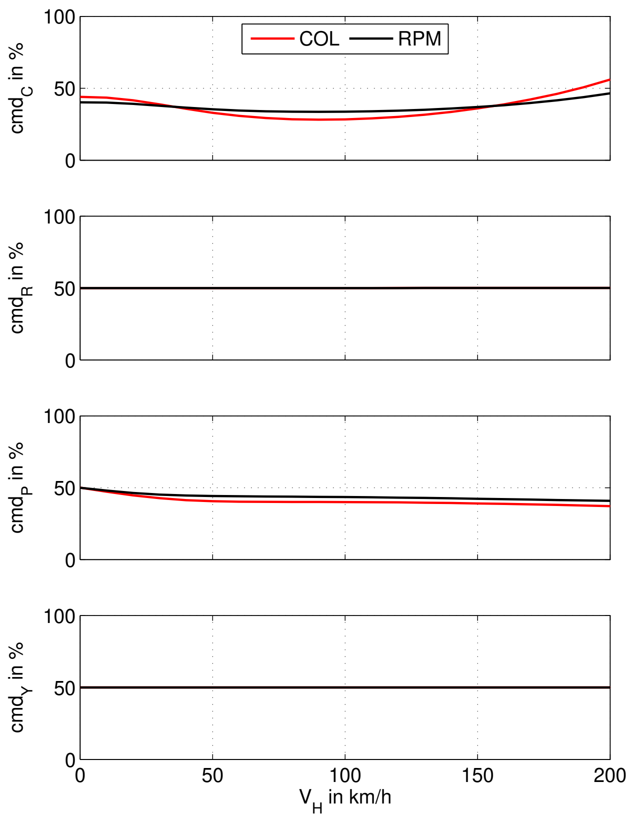

Figure 7 Control input versus horizontal flight speed

4.2. Flight Dynamics

To assess the flight dynamics using stability derivatives, a linear quadrotor model is needed. After the initial trim, the non-linear models are numerically linearized around the trim condition. The linearized model structure is given in state space form by

$$\dot{\overline{x}} = \mathbf{A}\overline{x} + \mathbf{B}\overline{u}$$
$$\overline{y} = \mathbf{C}\overline{x} + \mathbf{D}\overline{u} \tag{6}$$

where the state vector $\overline{x}$ given by Eq. (7), and it contains velocities, rates as well as attitude angles. $\mathbf{A}$ is the system matrix and $\mathbf{B}$ is the input matrix. $\mathbf{C}$ is the output matrix, defined by the identity matrix, where $\mathbf{D}$ is the feed-forward matrix, given by the zero matrix.

$$\overline{x} = \begin{bmatrix} u & v & w & p & q & r & \phi & \theta & \psi \end{bmatrix}^{\mathsf{T}} \tag{7}$$

Following the numerical linearization, the system matrix $\mathbf{A}$ given by Eq. (8) is obtained.

$$\mathbf{A} = \begin{bmatrix} X_u & 0 & 0 & 0 & X_q & 0 & 0 & X_\theta & 0 \\ 0 & Y_v & 0 & Y_p & 0 & 0 & Y_\phi & 0 & 0 \\ 0 & 0 & Z_w & 0 & 0 & 0 & 0 & 0 & 0 \\ 0 & L_v & 0 & L_p & 0 & 0 & 0 & 0 & 0 \\ M_u & 0 & 0 & 0 & M_q & 0 & 0 & 0 & 0 \\ 0 & 0 & 0 & 0 & 0 & N_r & 0 & 0 & 0 \\ 0 & 0 & 0 & 1 & 0 & 0 & 0 & 0 & 0 \\ 0 & 0 & 0 & 0 & 1 & 0 & 0 & 0 & 0 \\ 0 & 0 & 0 & 0 & 0 & 1 & 0 & 0 & 0 \end{bmatrix} \tag{8}$$

The entries represent the stability derivatives for their respective states, indicated by subscripts. Small entries with negligible effect on the flight dynamics were replaced by 0. A detailed description of these derivatives can be found in [13]. It should be noted that there are no longitudinal or lateral moments due to roll L_ϕ or pitch angle M_θ present in the system. These derivatives typically arise with introduction of attitude command-attitude hold (ACAH) response-type feedback and therefore are absent from bare airframe rotorcraft models.

Calculating the eigenvalues of the system without any control input ($\overline{u} = \overline{0}$) yield the poles of the system, which in turn reveal information about the dynamic modes. The poles of the COL- and RPM-variants in hover are shown in Fig. 8.

In total, there are five stable poles located on the real axis. Besides the integrator pole at the origin, these modes describe the reaction of the vehicle following yaw or heave perturbation as well as pitch and roll subsidence. As it is normal for all rotorcraft, the open-loop dynamics exhibit oscillatory unstable modes for perturbations in roll and pitch, which is known as the phugoid motion. Moreover, the roll and pitch subsidence are more significant, meaning that changes in attitude around these axes are more damped.

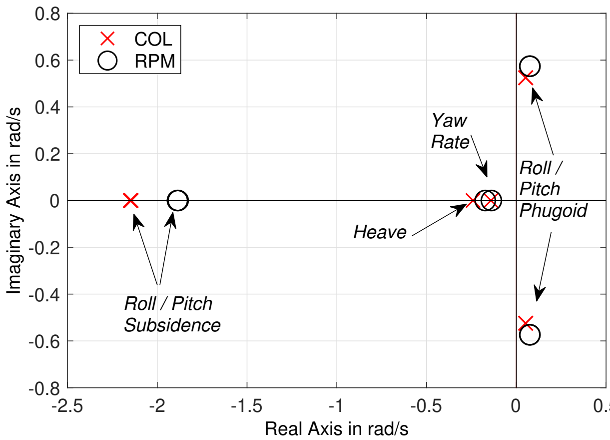

Figure 8 Location of the poles in hover

The pole placement for the yaw rate and heave mode are similar for both variants. It can be seen that the COL-variant exhibits a higher roll/pitch subsidence than the RPM-variant. As for the phugoid, the pole map suggests close motion characteristics for both variants, where the COL-variant is less oscillatory and more damped. Overall, it is expected to see close flight dynamics for both variants, with the COL-variant being slightly more stable than the RPM-variant.

5. HANDLING QUALITIES ASSESSMENTS

5.1. Predicted Handling Qualities

In order to make the initial HQs predictions, piloted frequency sweeps, step and pulse inputs were performed in AVES running the non-linear model in real time. The results were evaluated with respect to following ADS-33 HQ criteria:

- **Bandwidth/Phase Delay** is used to asses the vehicle response to inputs with small amplitudes and moderate to high frequencies.
- **Dynamic Stability** addresses the response characteristics for small amplitude and low to moderate frequency inputs.
- **Attitude Quickness** describes the response to large amplitude and low to moderate frequency inputs.
- **Axes Coupling** assesses the off-axis response due to pitch or roll attitude changes.
- **Height Response** describes the vertical rate response within 5 seconds following a step collective input.

The HQs for pitch and roll were assessed through the first four mentioned criteria. For yaw and heave, bandwidth, height response and axis coupling were considered. Further details on the given criteria can be found in the ADS-33E-PRF [8].

The predicted HQs are evaluated in three levels. Level 1 HQs stipulate that desired performance should be achievable without the moderate pilot compensation. HQs in Level 2 stipulate that deficiencies warrant improvement and it should be expected that required compensation will increase with respect to vehicles with Level 1 HQs. Level 3 HQs dictate that deficiencies require improvement and will likely indicate that the HQs are not sufficient to complete desired missions. As the results obtained are included in Appendix A with respect to ADS-33 prediction boundaries, Fig. 9 summarizes these results in a radar chart. The radar chart consists of three spokes. The outer spoke represents Level 3, the middle spoke Level 2 and the inner spoke Level 1 HQs for a given criterion.

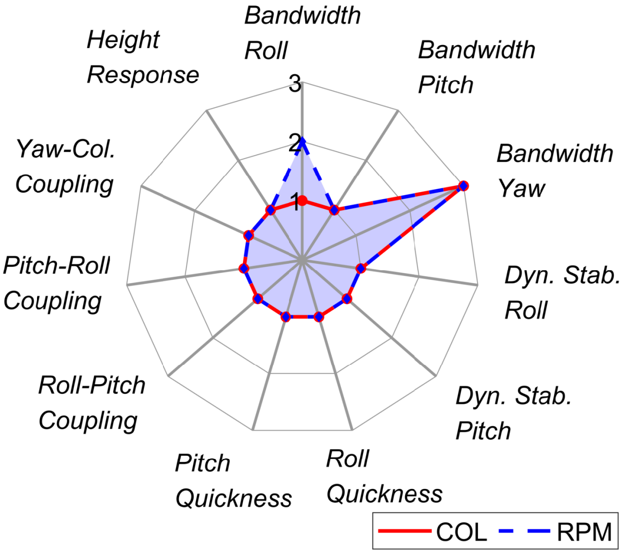

Figure 9 Predicted HQs of COL- and RPM-variants

Roll & Pitch

The pitch bandwidth was found to be within the Level 1 region for both variants, whereas the roll bandwidth was found to be Level 2 for the RPM-variant. This indicates a higher proneness to instability for the pilot-aircraft interaction: As the natural phase lag, introduced by the pilot reaction time, rises, the phase crossover frequency will be reached earlier for the RPM-variant. In this case (as is typical for a wide range of systems), the phase bandwidth is the limiting parameter for the overall bandwidth determination, meaning that the RPM-variant response will hit the -135° phase at a lower frequency than the COL-variant. This behavior is assumed to be caused by the time needed to raise and lower the rotational speed of the rotors compared to the fast change in the angle of attack for the collective control approach.

The dynamic stability criterion locates both variants within Level 1 boundaries, which is consistent with the pole placement resulting from desktop analysis (see Fig. 8). Attitude quickness falls within Level 1, meaning the models are able to generate desired damping in roll & pitch during moderate to large attitude changes. Pitch due to roll and roll due to pitch couplings are low. These couplings arise typically due to the gyroscopic and aerodynamic moments induced by the main rotor [14]. As the lift is distributed to multiple rotors symmetrically, it is presumed that roll moments resulting from the non-uniform inflow distribution on the rotor disks are canceled out for the most part and will be further investigated in future works.

Overall, the evaluation of the HQ criteria suggests a predicted HQ within Level 2 for roll and pitch, where the lateral axis is determined to be the most critical.

Yaw & Heave

The yaw bandwidth criterion locates both variants in the Level 3 region. This means that even for pedal input frequencies (e.g. slow direction changes), significant control lead with high gains would be expected in order to achieve the desired tracking performance. This issue addresses a lack of generated torque moment along the vertical axis over the corresponding moment of inertia, causing to insufficient yaw acceleration. Except for the absence of lateral forces (e.g. generated by the tail rotor), this problem can be triggered by two main reasons in the studied configurations: insufficient rotor rotational inertia or low yaw calibration in the $\mathbf{G}$ matrix (see Section 3).

The acceleration along the vertical axis is achieved by lowering or raising the thrust command R for all rotors simultaneously. Thanks to the symmetric rotor positioning and the identical number of counter-rotating rotors, the moment balance is inherently achieved on the fuselage. This results in decoupled yaw and heave axis when thinking about main rotor-tail rotor configurations.

Overall, due to the low bandwidth of the yaw axis, the aircraft is predicted to have Level 3 HQs for yaw & heave.

5.2. Awarded Handling Qualities

A piloted simulation campaign was conducted to perform an initial evaluation of the models investigated. The tests were conducted in the Air Vehicle Simulator (AVES) with nonlinear time domain computations were run by HOST in the background.

As no generic or eVTOL cockpit is available in AVES, the EC-135 cockpit was used for the tests. Although it is not representative for the proposed eVTOL designs, the helicopter cockpit was considered adequate for the initial test campaign. To represent the studied configuration in the simulator, an eVTOL external visual model with a high-aft rotor arrangement was chosen (see Fig. 10a). With the forward rotors being visible within the cockpit sight (Fig. 10b), it was intended to give the pilots a higher perception of flying in a quadrotor rather than sitting in a helicopter cockpit.

The tests were conducted under ideal weather conditions. No stability augmentation or protection system was used during the tests in order to asses the bare airframe characteristics. In addition, the motion system was not used for the test campaign, as motioned simulator flights are planned for the future work.

The flight tests were performed with two experimental helicopter pilots at DLR. The pilot experience is summarized in Table 3.

	License Years	Flight Hours	Type Ratings
Pilot A	41	6700	EC-135, Bo 105, CH-53, Bell UH-1D
Pilot B	12	1050	EC-135, Bo 105, Bell 205, Bell 412, Alouette II

Table 3 Pilot overview

From the mission task elements (MTEs) available in ADS-33, four were selected, as they are considered suitable for the CONOPS of future eVTOL quadrotor aircraft:

- **Hover:** 45° diagonal approach towards the final position and stabilize in hover.
- **Hover Turn:** 180° turn over the reference position in both directions.
- **Pirouette:** Translation around a circular circumference with the aircraft nose pointing at the center of the circle.
- **Slalom:** S-shaped maneuvers over a straight line by flying through positioned gates.

It is acknowledged that these MTEs are not suitable for all types of eVTOL configurations, particularly for those not required to hover for long periods. In this regard, initial efforts to define similar MTEs for eVTOL aircraft are ongoing, both in Europe (SC-VTOL) and the United States [15], [16]. Since these efforts are not currently mature enough to be used in evaluations for this initial study, ADS-33 maneuvers were directly used. All MTEs were flown according to requirements for cargo/utility aircraft for good visual conditions as classified in ADS-33. It was considered that scout/attack requirements do not reflect future mission requirements of an eVTOL aircraft.

Prior to awarding the MTEs, pilots performed free-flights with the models about 10 to 15 minutes. During these warm-up flights, pilots developed a sense of representative strategy to control the quadrotor variants. Once the desired sense of control strategy was reached, the MTEs were flown sequentially for each configuration. Prior to execution of each test, the pilots were shortly briefed about the description and objectives of the particular MTE. The pilots awarded the Handling Qualities Ratings (HQRs) using the Cooper-Harper scale [17], following the completion of each MTE.

The Cooper-Harper scale provides a simplified evaluation process to the pilot to rate the adequacy of the aircraft handling qualities by going through simple questions. Depending on the given answers with *yes* or *no*, the handling qualities are rated from 1 to 10, corresponding to the following adequacy groups:

- **1-3:** Acceptable and satisfactory,
- **4-6:** Acceptable but unsatisfactory,
- **7-9:** Unacceptable,
- **10:** Unflyable.

In ADS-33, Level 1 and Level 2 handling qualities are directly related to aforementioned first two groups, where Level 3 ranges from 7 to 8, excluding 9 and 10. Table 4 shows the HQRs given by the both pilots for COL- and RPM-variants. It has to be mentioned that two MTEs were not flown during the tests for the COL-variant. These are Slalom for Pilot A and Hover Turn for Pilot B.

Fig. 11 shows a graphical overview of the results. Here, the flown MTEs are placed in the horizontal axis, where the vertical axis shows the HQRs with respect to Cooper-Harper rating scale. The horizontal dashed lines show the borders of the handling qualities levels prescribed in the ADS-33. For each MTE and control variant, the ratings are shown through bars ranging between the extreme ratings with the label icons placed in the middle. Here, MTEs rated for the COL-variant are labeled with circle and for the RPM-variant with rhombus.

(a) Outside view of the simulation

(b) Cockpit view of the simulation

Figure 10 Air Taxi model in AVES

	COL		RPM	
MTE	Pilot A	Pilot B	Pilot A	Pilot B
Hover	4	8	5	6
Hover Turn	4	-	7	6
Pirouette	4	6	6	5
Slalom	-	4	4	4

Table 4 HQRs of the Piloted Simulations (MTEs marked with **-** were not flown)

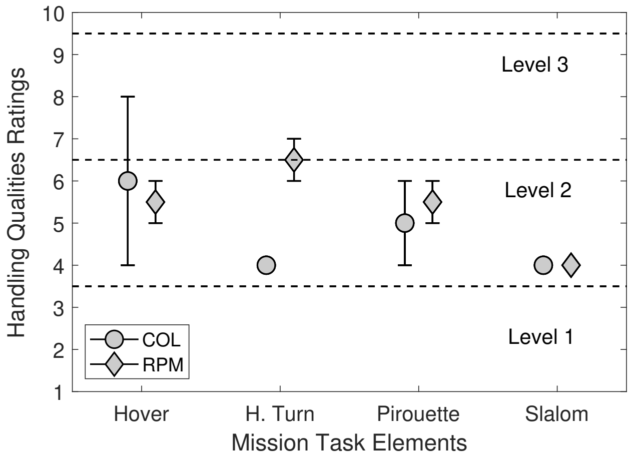

Figure 11 Handling qualities ratings of the flown MTEs

The results show that the HQRs were found within the Level 2/3 region. Although the quantitative criteria concerning pitch and roll axes were found to be either in Level 1 or close to the boundary, no MTE was awarded Level 1 due to high pilot-in-the-loop oscillations (PIOs) experienced throughout the flight tests.

In the Hover MTE, the large separation between the ratings of both pilots for the COL-variant was observed. This shows the difference in the control strategy of both pilots reacting to the vehicle attitude. The pilots stated that the high agility in roll and pitch responses of both variants led to difficulties to stabilize the vehicle during the deceleration segment of the MTE. Here, the pilots experienced large oscillations during the deceleration, as a result of lateral and longitudinal compensation inputs.

The Hover Turn MTE for the COL-variant was awarded HQR 4 (Level 2), indicating that the desired performance could be achieved. For the RPM-variant, ratings in the Level 2/3 region were awarded, indicating a strong degradation in HQs with respect to the former case. The main aspect that contributed to awarded ratings was the poor bandwidth in the yaw axis, requiring aggressive pedal inputs and compensation afterwards. In addition, stick inputs for further compensation in the lateral and longitudinal axis caused the aircraft the shift off of the reference point, which had to be compensated with more control inputs. Nevertheless, problems related to oscillations and control difficulty were not as prevalent as in the Hover MTE.

Moreover, it is worthy to mention that the awarded ratings imply better characteristics in the yaw handling than the predicted yaw bandwidth found to be in Level 3. Since the HQ prediction criteria in the ADS-33 are mainly designed for the standard main rotor-tail rotor arrangement, the decoupling between yaw and heave in quadrotors can exceptionally exhibit better yaw handling in the flight tests than what is predicted. This issue will be investigated in more detail in the future work.

The Pirouette MTE was awarded Level 2 HQs. Here, the poor yaw bandwidth led to high workload maintaining the required heading. Both models required less compensations in this MTE, compared to previous two, since the maneuver was a low speed steady circular translation. Furthermore, unlike in the main rotor-tail rotor configurations, the lack of cross-couplings made it easier to complete the task to adequate performance standards.

The Slalom was the only MTE where both pilots awarded HQR 4 (Level 2) for both configurations, indicating that desired performance was obtained. Here, the pilots did not report extreme difficulties from the high agility in roll and pitch attitude.

It is worthy to mention that pilot observations concerning the COL- and RPM-variants showed inconsistency, resulting from the strategies employed by the pilots. Pilot A had larger problems stabilizing the oscillations in the RPM-variant, whilst for Pilot B, this occurred for the COL-variant. This problem was not observed through the quantitative ADS-33 criteria applied. Two possibilities are considered here; either the criteria from ADS-33 has been overlooked to expose this deficiency or additional refinements in the criteria used are required for the assessment of eVTOL aircraft. This will be investigated in future work.

6. CONCLUSIONS

A two passenger quadrotor configuration with variable blade pitch and variable rotor speed control variants were investigated. A mathematical formulation between the quadrotor vehicle control and the conventional inceptor layout was introduced that is suitable for both control variants. The models were primarily analyzed regarding trim performance and flight dynamics. The HQs were assessed based on various criteria and MTEs provided by ADS-33E-PRF. The awarded handling qualities were obtained through flight tests conducted at DLR's flight simulator facility AVES with experimental helicopter pilots. Following conclusions were found:

- The quadrotor configuration exhibits unstable flight characteristics in bare airframe, regardless control variant.
- Unstable lateral and longitudinal phugoid modes and low yaw rates were found to be critical during flight dynamics and HQ assessments. Based

on these issues, the flight models require further enhancements.

- Despite predicted HQs mostly found to be in Level 1, no MTE was awarded Level 1 by the pilots. Moreover, despite the Level 3 HQs was predicted by the yaw bandwidth criterion, the Hover Turn MTE was awarded Level 2 by the pilots.
- The inconsistency between the predicted and awarded HQs shows that the prediction criteria given in the ADS-33 are not well suited for the assessments of unconventional multirotor configurations and reveals the need for new standards.

Future works will concentrate on the enhancement of the handling qualities of the quadrotors studied in terms of active and passive improvements. The former will feature the use of stability augmentation system (SAS), where the latter will investigate the constructive approaches, such as blade design optimization, and new rotor arrangements. Moreover, full-motion flight tests are planned in AVES to increase the realism of the test environment for the pilots.

Contact address:

kagan.atci@dlr.de

References

[1] Kenneth I. Swartz. Charging forward: new evtol concepts advance. *Vertiflite*, July/August 2017.

[2] Gregor Grandl, Martin Ostgathe, Jan Cachay, Stefan Doppler, John Salib, and Han Ross. The future of vertical mobility-sizing the market for passenger, inspection, and goods services until 2035 - a porsche consulting study. 2018.

[3] Shannah Withrow-Maser Carlos Malpica. Handling qualities analysis of blade pitch and rotor speed controlled evtol quadrotor concepts for urban air mobility. In *VFS International Powered Lift Conference 2020*, San Jose, CA, January 2020.

[4] Michael J. Duffy, Sean R. Wakayama, and Ryan Hupp. A study in reducing the cost of vertical flight with electric propulsion. In *17th AIAA Aviation Technology, Integration, and Operations Conference*, page 3442, Denver, CO, June 2017.

[5] Christopher Silva, Wayne R. Johnson, Eduardo Solis, Michael D. Patterson, and Kevin R. Antcliff. VTOL urban air mobility concept vehicles for technology development. In *2018 Aviation Technology, Integration, and Operations Conference*. American Institute of Aeronautics and Astronautics, June 2018. DOI: 10.2514/6.2018-3847.

[6] Wayne Johnson, Christopher Silva, and Eduardo Solis. Concept vehicles for vtol air taxi operations. In *AHS Conference on Aeromechanics Design for Transformative Vertical Flight*, January 2018.

[7] Peter Weiand, Michel Buchwald, and Dominik Schwinn. Process development for integrated and distributed rotorcraft design. *Aerospace*, 6(2):23, February 2019. DOI: 10.3390/aerospace6020023.

[8] United States Army Aviation and Missile Command Aviation Engineering Directorate. Ads-33e-prf aeronautical design standard performance specification handling qualities requirements for military rotorcraft. Technical report, Redstone Arsenal, Alabama, March 2000.

[9] Carsten M. Liersch and Martin Hepperle. A distributed toolbox for multidisciplinary preliminary aircraft design. *CEAS Aeronautical Journal*, 2(1-4):57–68, August 2011. DOI: 10.1007/s13272-011-0024-6.

[10] Martin Siggel, Jan Kleinert, Tobias Stollenwerk, and Reinhold Maierl. TiGL: An open source computational geometry library for parametric aircraft design. *Mathematics in Computer Science*, 13(3):367–389, July 2019. DOI: 10.1007/s11786-019-00401-y.

[11] B. Benoit, A.-M. Dequin, K. Kampa, W. von Grünhagen, P.-M. Basset, and B. Gimonet. Host, a general helicopter simulation tool for germany and france. In *American Helicopter Society, 56th Annual Forum and Technology Display*, Virginia Beach, VA, May 2000.

[12] Holger Duda, Sunjoo K. Advani, and Mario Potter. Design of the DLR AVES research flight simulator. In *AIAA Modeling and Simulation Technologies (MST) Conference*, page 4737, Boston, MA, August 2013. DOI: 10.2514/6.2013-4737.

[13] Robert J. Niemiec and F. Gandhi. A comparison between quadrotor flight configurations. In *42nd European Rotorcraft Forum*, Lille, France, September 2016.

[14] Gareth D. Padfield. *Helicopter flight dynamics: the theory and application of flying qualities and simulation modelling*. Blackwell Pub. American Institute of Aeronautics and Astronautics, Oxford Washington DC, 2007. ISBN: 9781405118170.

[15] European Union Aviation S. Second publication of proposed means of compliance with the special condition vtol. Technical report, 2021.

[16] David H. Klyde, Philip C. Schulze, David G. Mitchell, David Sizoo, Ross Schaller, and Robert McGuire. Mission task element development process: An approach to faa handling qualities

certification. In *AIAA Aviation 2020 Forum*, page 3285, 2020.

[17] George E. Cooper and Robert Harper. The use of pilot ratings in evaluation of aircraft handling qualities. NASA Technical Note TN D-5153, NASA, Ames Research Center Moffett Field, CA, 1969.

A. HANDLING QUALITIES PREDICTIONS

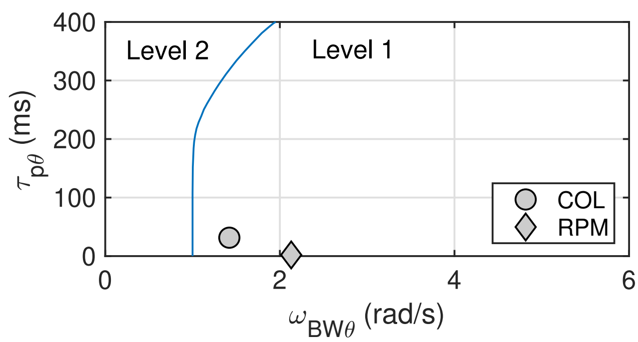

(a) Pitch *(All other MTEs - UCE=1 and fully attended operations)*

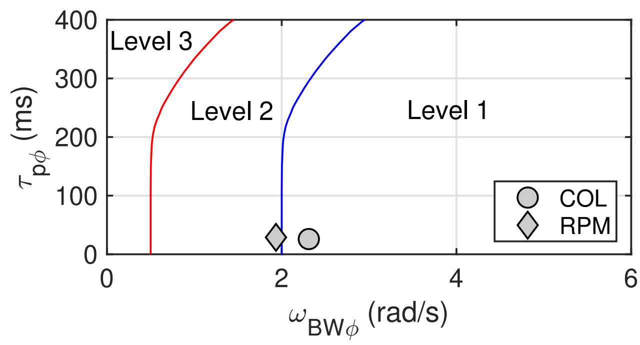

(b) Roll *(All other MTEs - VMC, UCE=1 and fully attended operations)*

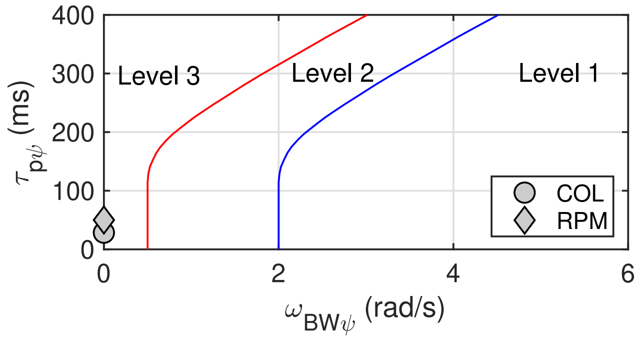

(c) Yaw *(All other MTEs - hover and low speed)*

Figure 12 Bandwidth

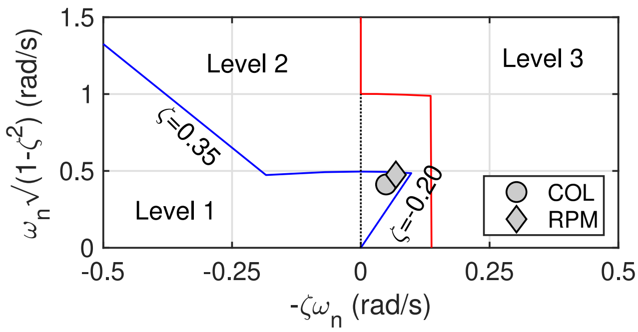

(a) Pitch *(Fully attended operations in Hover)*

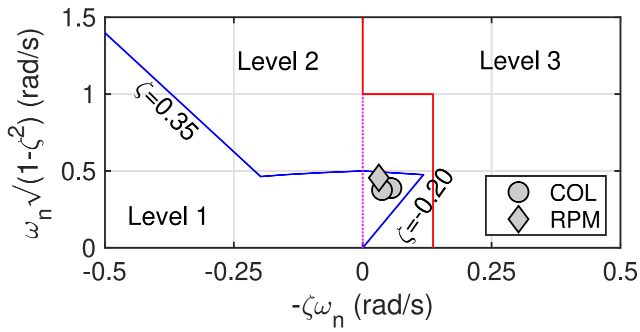

(b) Roll *(Fully attended operations in Hover)*

Figure 13 Dynamic stability

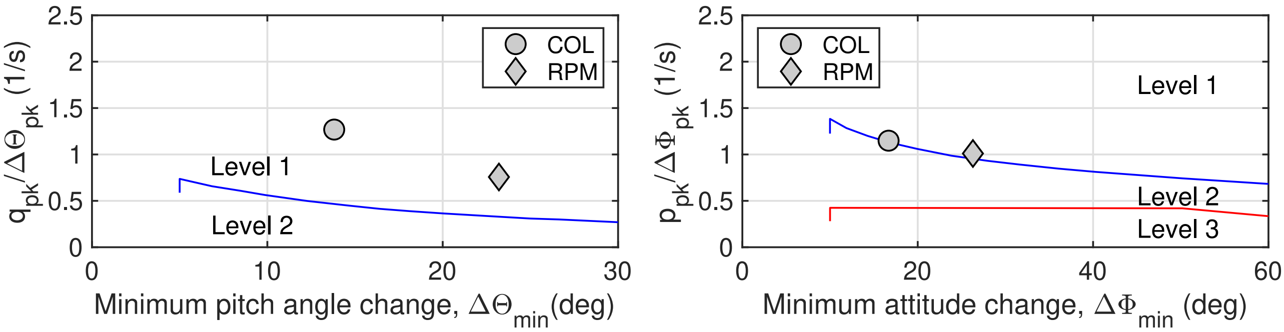

(a) Pitch

(b) Roll

Figure 14 Attitude quickness

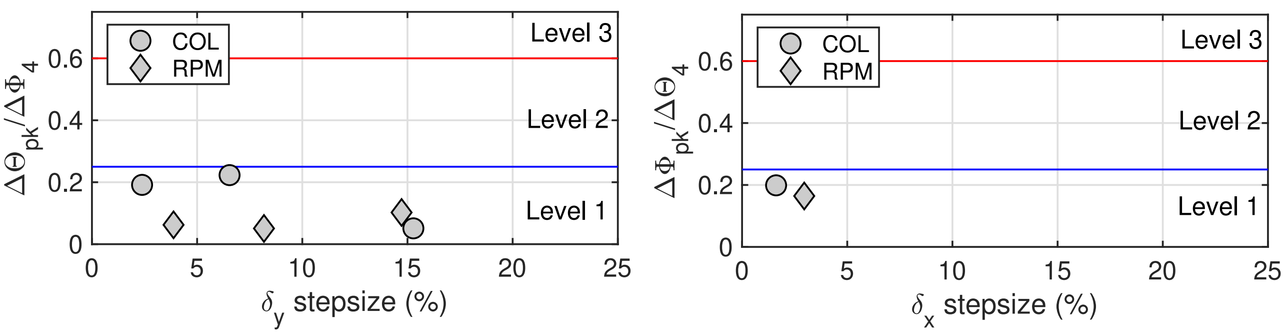

(a) Pitch coupling due to roll

(b) Roll due to pitch

Figure 15 Cross-couplings between pitch and roll

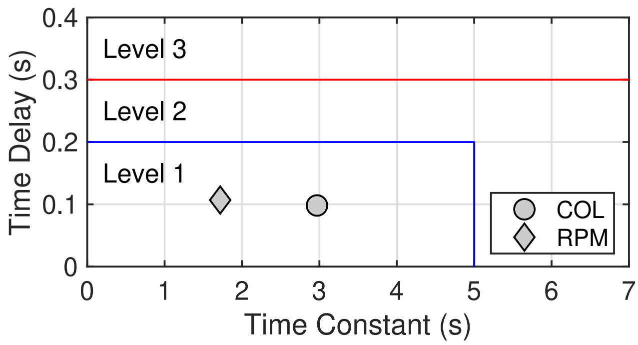

Figure 16 Height response

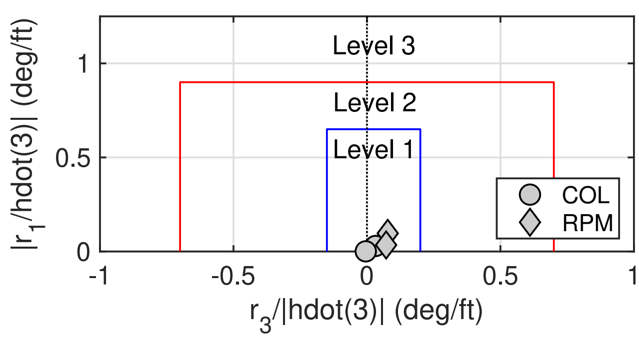

Figure 17 Yaw-due-to-collective coupling